



Cite this: *RSC Adv.*, 2024, 14, 24019

Ruthenium complexes with triazenide ligands bearing an N-heterocyclic moiety, and their catalytic properties in the reduction of nitroarenes†

Christian A. Romero-Soto,^{§a} Ana L. Iglesias,^{§b} Amor F. Velázquez-Ham,^a Juan P. Camarena-Díaz,^a Erick Correa-Ayala,^a Jessica L. Gomez-Lopez,^a Daniel Chávez,^a Adrián Ochoa-Terán,^{§a} Gerardo Aguirre,^a Arnold L. Rheingold,^c Douglas B. Grotjahn,^{§d} Miguel Parra-Hake^a and Valentin Miranda-Soto^{§*a}

A series of ruthenium complexes of formulae [RuCl(triazenide)(*p*-cymene)] have been synthesized using as ligand a triazenide monofunctionalized with an N-heterocyclic moiety. Nuclear magnetic resonance, high resolution mass spectrometry and X-ray diffraction were used to characterize the triazenide ligands and their complexes. In addition, these ruthenium complexes catalyzed the reduction of nitrobenzene to aniline in the presence of sodium borohydride and ethanol as solvent at room temperature. Notably, complex **5** was especially active in the reduction of nitroarenes substituted at the aromatic ring with electron-withdrawing or electron-donating functional groups affording the desired arylamines in good to excellent yields (80–100%). The role of the N-heterocyclic moiety on catalysis was explored.

Received 2nd July 2024
Accepted 19th July 2024

DOI: 10.1039/d4ra04813j

rsc.li/rsc-advances

Introduction

Aryl amines are an important motif found in the structure of many significant molecules used as dyes, pharmaceuticals, and agrochemicals.¹ The most straightforward methodology to obtain aryl amines is a two-step pathway that includes nitration of arenes and subsequent reduction of nitroarenes.² The use of iron, ferrous salts, or iron catalysts in aqueous acid is a chemical process, referred as the Béchamp reduction, which has been used in order to achieve the reduction of nitroarenes to the corresponding aryl amines.³ However, the main drawback of this methodology is the production of a lot of metallic waste along with the elevated temperature required for an efficient reduction.^{4a,g} In contrast, catalytic hydrogenation is a green methodology for reduction of nitroarenes that has been

extensively reviewed in the last decade.⁴ These methodologies are predominantly based on heterogeneous catalysis, and have been classified based on the source of hydrogen utilized during the reduction and the mechanism involved in the process. In comparison, homogeneous catalytic systems have been less studied, probably due to some disadvantages associated with their industrial application. Nevertheless, there are several examples of homogeneous catalysts based on iron,⁵ cobalt,⁶ nickel,⁷ molybdenum,⁸ manganese,⁹ palladium,¹⁰ rhodium,¹¹ and ruthenium complexes.¹² Among these, ruthenium complexes stand out for being able to reduce nitroarenes using as hydrogen source sodium borohydride, hydrogen gas or alcohols. In the sodium borohydride methodology, the ligands more frequently found in the ruthenium complexes are imines, amide-phosphines, aryloxazolines, and quinolates. These are five or six-membered chelating ligands with N–O or N–C coordinating atoms. However, there are no examples for the reduction of nitroarenes performed by ruthenium complexes containing four-membered chelating ligands with N–N atom donors, bearing a pendant-heterocyclic base. Exploring the

^aTecnológico Nacional de México/Instituto Tecnológico de Tijuana/Centro de Graduados e Investigación en Química, Blvd. Alberto Limón Padilla S/N, 22454 Tijuana, BC, Mexico. E-mail: vmiranda@tectijuana.mx

^bFacultad de Ciencias de la Ingeniería y Tecnología, Universidad Autónoma de Baja California, Mexico

^cDepartment of Chemistry and Biochemistry, University of California at San Diego, CA 92093, USA

^dDepartment of Chemistry and Biochemistry, San Diego State University, CA 92182, USA

† Electronic supplementary information (ESI) available. CCDC 2087352 (5), 2087431 (6), 2087433 (7), 2284161 (12), 2284162 (13). For ESI and crystallographic data in CIF or other electronic format see DOI: <https://doi.org/10.1039/d4ra04813j>

§ These authors contributed equally to the work.

‡ Deceased.

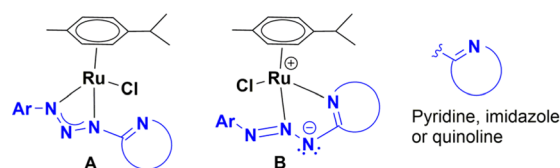


Chart 1 Four (A) and five-membered (B) chelating triazenide ligands in ruthenium complexes.



catalytic properties of iridium, rhodium and ruthenium–triazene complexes¹³ in the transfer hydrogenation of unsaturated molecules, we envision that either complex **A** or **B**, with the triazene bearing an N-heterocyclic moiety, could be useful in the reduction of nitroarenes. Therefore, in this work, we report the structural characterization, catalytic behaviour, and reactivity of four ruthenium complexes with triazene ligands bearing an N-heterocyclic moiety (Chart 1).

Results and discussion

Precursors of triazene ligands functionalized with heterocycles like pyridine **1** and quinoline **2** were synthesized by the traditional procedure of N-coupling of diazonium salts (Scheme 1).^{14,15} Triazenes **1** and **2** were fully characterized by spectroscopic techniques. On the other hand, ligands **3** and **4** functionalized with imidazole moieties have been previously reported by our group^{13b} and were synthesized by the reaction of 2-lithioimidazoles with 4-azidotoluene, followed by hydrolysis.

The ¹H NMR spectra of triazenes **1** and **2** show the characteristic NH signal of the diazoamine group as a broad singlet at 11.51 and 13.12 ppm, respectively. The expected A₂B₂ system for the aromatic rings is observed for **2** as two doublets at 7.52 and 7.63 ppm (*J* = 8.6 Hz), whilst for **1**, the signal for proton H4 of the pyridine ring overlaps with one of the A₂B₂ signals and has the appearance of a triplet centered at 7.54 ppm. The resonances for the aromatic protons of pyridine and quinoline

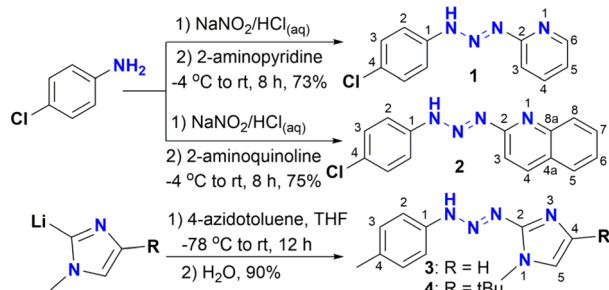
rings are observed in the region of 6.97–8.93 ppm and 7.45 to 8.34 ppm, respectively.

The ¹³C {¹H} NMR spectra of compounds **1** and **2** show the typical signals for aromatic carbons from 109.0 to 154.7 ppm and 110.5 to 153.9 ppm, respectively. Interestingly, for triazene **1**, the aromatic carbon C1 is absent from both ¹³C {¹H} NMR and APT spectra, even if other NMR solvents are used in its analysis. Finally, running a ¹³C proton-coupled NMR experiment shows the signal as a singlet at 148.2 ppm, which is under the signal for carbon C6 of the pyridine ring in the regular ¹³C experiment (Fig. S5 and S6†).

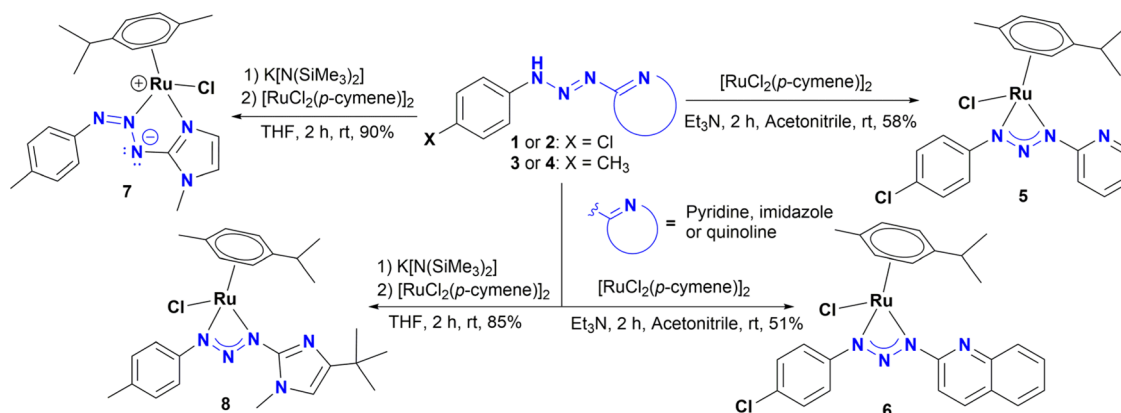
Ruthenium(II) triazene complexes

Reaction of ligand precursors **1** or **2** with one half equivalent of [RuCl₂(*p*-cymene)]₂, in acetonitrile at room temperature in the presence of triethylamine, resulted in the formation of new half sandwich Ru(II) complexes **5** and **6** (Scheme 2). These compounds were isolated as air and moisture stable micro-crystalline orange solids. On the other hand, complexes **7** and **8** were synthesized using a different methodology according to Scheme 2. Treatment of a solution of **3** or **4** in dry THF with K[N(SiMe₃)₂] led to the formation of potassium triazene, which can be directly converted into complexes **7–8** by a trans-metallation reaction with [RuCl₂(*p*-cymene)]₂. All complexes were characterized by ¹H NMR and ¹³C {¹H} NMR spectroscopy, HRMS, and single crystal X-ray diffraction analysis. The assignments are supported by ¹H–¹H gCOSY, ¹H–¹³C gHSQC and ¹H–¹³C gHMBC correlation experiments. The ¹H and ¹³C {¹H} NMR of complexes **5** and **6** show a very similar spectra, as can be expected from their proposed structures, and suggest a chiral environment around the ruthenium centre since the *p*-cymene aromatic protons appear as four distinct doublets in the region of 5.48 and 6.07 ppm (*J* = 5.6 Hz) for **5** (Fig. S34†).

These resonances are slightly shifted downfield in complex **6** due to the presence of the quinoline ring and appear in the region of 5.56 and 6.17 ppm when it is analysed in CD₂Cl₂ (Fig. S52†). For **6** in DMSO-*d*₆, the latter signals are slightly overlapped with an additional downfield shift of 5.83 to 6.23 ppm (Fig. S60†). Likewise, the isopropyl methyl protons of the *p*-cymene are not equivalent and appear as two doublets at



Scheme 1 Synthesis of triazenes **1–4**.



Scheme 2 Synthesis of complexes **5–8**.



1.25 and 1.26 ppm ($J = 6.4$ and 6.9 Hz) for both **5** and **6**. This behaviour has been observed in related asymmetric Ru(II)(*p*-cymene) complexes.^{12d,f-h,13d} Interestingly, analysing the microcrystalline solid in solution by ^1H NMR showed **6** as the major species along another minor species ($\sim 10\%$) with a similar set of NMR resonances, which may be a coordination isomer of **6** (Fig. S53†).

In general, for compounds **5** and **6**, all ^1H NMR signals are slightly shifted up field compared to the free ligand **1** and **2** (Fig. S45 and S61,† respectively). However, an interesting feature in complexes **5** and **6** is the appearance of the aromatic A_2B_2 system, which exhibits a second-order effect and is observed as a multiplet centered at 7.11 for **5**, and 7.37 ppm for **6** (with $\Delta\nu/J = 1.9$ and 1.6 Hz), respectively. The $^{13}\text{C}\{^1\text{H}\}$ NMR analysis of **5** and **6** corroborated the asymmetric nature of the complexes. The spectrum shows six signals for the aromatic *p*-cymene carbons, which are seen between 79.8 and 103.1 ppm for **5** and 80.3 and 103.7 ppm for **6**, as well as the two diastereotopic methyl carbons of the *i*Pr group, which appear between 22.7 and 23.0 ppm for both complexes (Fig. S35, S36 and S54†). In addition, the carbon resonances (C2) of the heterocyclic moieties in complexes **5** and **6** are shifted downfield (~ 4 ppm) in comparison with the C2 in triazenes **1** and **2**. In contrast, there is a slight up-field shift (≥ 2.10 ppm) of the aryl carbon resonances (C1) for **5** and **6**, compared to the free triazenes **1** and **2**.

The ^1H NMR and ^{13}C NMR spectra of **8** are similar to those of complexes **5** and **6**, suggesting the same coordination mode. Particularly, the signals for the *p*-cymene protons also appear as four doublets in the region of 5.50 and 6.04 ppm ($J = 5.9$ Hz), as well as two doublets ($J = 7.0$ Hz) for the methyl groups of the *i*Pr at 1.28 and 1.30 ppm (Fig. S75†). However, the splitting pattern for the aromatic hydrogens is different. For **8** the A_2B_2 system is clearly observed as two doublets at 7.10 and 7.22 ppm ($J = 8.3$ Hz), in agreement with related Ir(III) and Rh(III) triazenide complexes.^{13a,b} In addition, three singlets are observed at 3.52, 2.29 and 1.29 ppm, which are assigned to $\text{N}-\text{CH}_3$, ^tBu and $\text{H}_3\text{C}-\text{Ph}$, respectively. In contrast, the signals for the *p*-cymene ring in **7** are quite different from all other complexes, which suggests a different coordination mode. Thus, the A_2B_2 system of the *p*-cymene collapses into a pseudotriplet centered at 5.66 ppm and a slightly broad multiplet at 5.38 ppm, whereas the methyl groups of the *i*Pr give only one doublet at 1.19 ppm ($J = 6.9$ Hz) (Fig. S69†). Moreover, as observed in complex **8**, the signals for the A_2B_2 system of the aromatic ring for **7** also appear as two doublets at 7.75 and 7.12 ppm ($J = 8.3$ Hz). Lastly, the proton resonance for the imidazole moiety appears as two doublets at 6.72 and 7.14 ppm ($J = 1.8$ Hz).

In the $^{13}\text{C}\{^1\text{H}\}$ NMR spectrum for **8**, the *p*-cymene CH carbons appear between 80.0 and 81.7 ppm. However, the same resonances for complex **7** are shifted downfield to 83.1 and 87.6 ppm compared to all other complexes. These differences in chemical shifts might be a consequence of the coordination of the imidazole ring. Another fact that supports this assumption is the resonance of C5, which are shifted upfield at 117.6 ppm compared to 120.9 ppm in the free triazene **3** (151.0 ppm), as well as the significant downfield shift of C2 (161.2 ppm)

compared to the free ligand **3** (151.0 ppm). In contrast, there is no evidence for nitrogen–imidazole coordination in complex **8**, whose ^{13}C NMR data shows no significant changes in chemical shift of the C5 resonance (114.4 ppm) or in C2 (145.9 ppm) in comparison with the same signals in the free triazene **4** (114.1 and 146.8 ppm, respectively (Fig. S27 and S76†)).^{13b}

The molecular structures of compounds **5**–**7** were determined by X-ray diffraction analysis (Fig. 1–3). Complexes **5** and **6** crystallized in the orthorhombic crystalline system, while **7** in the monoclinic system with different space groups ($P2_12_12_1$ for **5** and **6**; $P2_1/n$ for **7**). These half sandwich Ru(II) complexes adopt a pseudo-octahedral “piano-stool” geometry with the *p*-cymene acting as the seat, a chloro ligand and the *N,N* donor atoms completing the coordination sphere. This three-legged structure is commonly observed in other related half-sandwich ruthenium *N,N* chelating ligand complexes.^{13c,d}

For complexes **5** and **6**, the metal coordinates through the terminal nitrogen atom forming a four-membered chelate with the bidentate triazenide ligand. The octahedral distortion in these compounds is caused primarily by the small-bite angle of the coordinating ligand, which is in the range of 58.47 and 59.16° , in agreement with other reported systems, while the $\text{N}-\text{Ru}-\text{Cl}$ angle is close to the expected 90° . The similar $\text{N}(2)-\text{N}(3)$ and $\text{N}(3)-\text{N}(4)$ bond distances in the triazenide (~ 1.31 to ~ 1.32 Å) indicates π -delocalization over the metal-triazenide system for **5** and **6**.¹⁶ In contrast, in complex **7** the ligand coordinates through $\text{N}(1)$ of the imidazole and $\text{N}(3)$ of the triazenide system, forming a five-membered chelate ring with a bite angle of $75.39(7)^\circ$ (Fig. 3).^{12b,13b,17} Furthermore, the $\text{N}(3)=\text{N}(4)$ double bond distance of $1.284(2)$ Å is comparable to analogous Rh(III) and Ir(III) Cp* half sandwich triazenide complexes, where the ligand is coordinated through the imidazole ring.^{13b}

The Ru–N bond lengths of complexes **5**–**7** are in the range of $2.067(3)$ Å to $2.103(2)$ Å, while the Ru–Cl bond distances are between $2.398(10)$ to $2.4195(6)$ Å, and are consistent with Ru–N

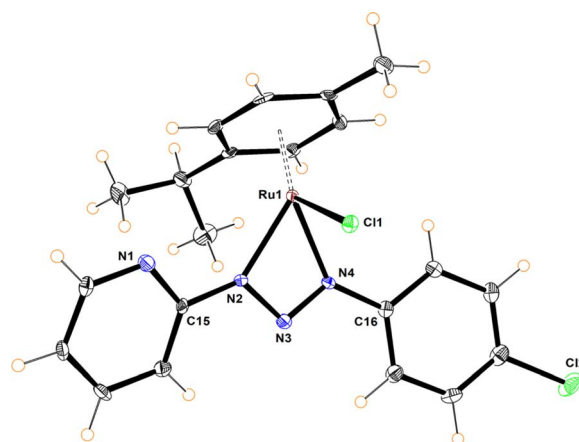


Fig. 1 Molecular structure of **5**. Selected bond distances (Å): $\text{N}(2)-\text{N}(3)$, 1.325(4); $\text{N}(3)-\text{N}(4)$, 1.320(4); $\text{Ru}(1)-\text{N}(2)$, 2.067(3); $\text{Ru}(1)-\text{N}(4)$, 2.081(4); $\text{Ru}(1)-\text{Cl}(1)$, 2.3985(10). Selected bond angles ($^\circ$): $\text{N}(2)-\text{Ru}(1)-\text{N}(4)$, $59.16(11)$; $\text{N}(2)-\text{Ru}(1)-\text{Cl}(1)$, $86.26(10)$; $\text{N}(4)-\text{Ru}(1)-\text{Cl}(1)$, $83.09(1)$; $\text{N}(2)-\text{N}(3)-\text{N}(4)$, $101.5(3)$.



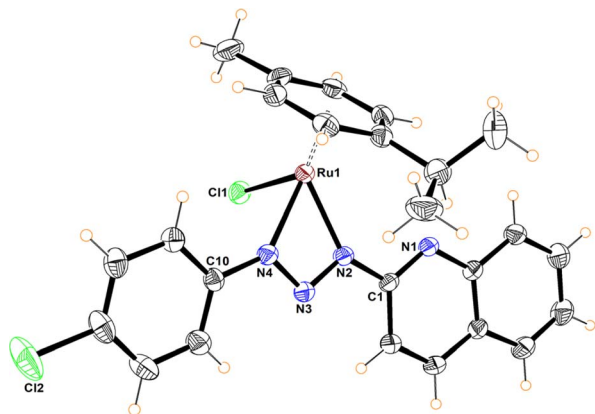


Fig. 2 Molecular structure of **6**. Selected bond distances (Å): N(2)–N(3), 1.316(5); N(3)–N(4), 1.301(5); Ru(1)–N(2), 2.081(4); Ru(1)–N(4), 2.101(4); Ru(1)–Cl(1), 2.398(1). Selected bond angles (°): N(2)–Ru(1)–N(4), 58.7(1); N(2)–Ru(1)–Cl(1), 88.1(1); N(4)–Ru(1)–Cl(1), 83.2(1). N(2)–N(3)–N(4), 103.1(4).

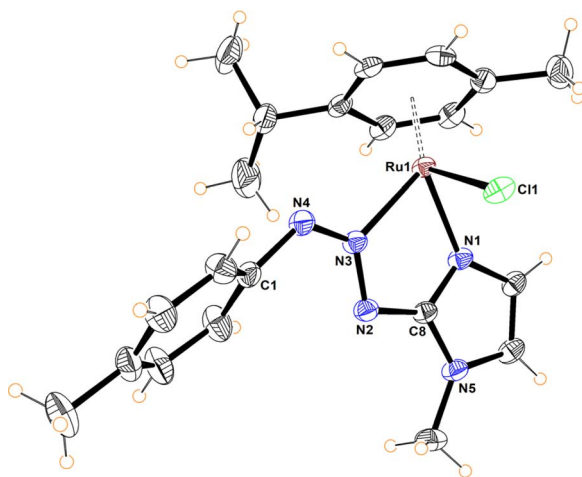


Fig. 3 Molecular structure of **7**. Selected bond distances (Å): N(3)–N(4), 1.284(2); N(2)–N(3), 1.348(2); N(3)–Ru(1), 2.103(2); N(1)–Ru(1), 2.053(2); Cl(1)–Ru(1), 2.4195(6). Selected bond angles (°): N(3)–Ru(1)–N(1), 75.39(7)°; N(3)–Ru(1)–Cl(1), 85.64(5); N(1)–Ru(1)–Cl(1), 84.17(5); N(2)–N(3)–N(4), 121.1(2).

and Ru–Cl1 bond length values reported for other half-sandwich ruthenium complexes with *N,N* ligands.^{13c,18}

Lastly, the most abundant peak in the HRMS (ESI-TOF) mass spectra of these complexes is generally associated with $[M + H]^+$, which is seen at 503.0327 (**5**), 553.0467 (**6**), 486.0967 (**7**), and 542.1615 (**8**) amu (Fig. S43, S67, S74, and S80,† respectively). In addition, for compounds **5** and **6** the spectra show the formation of the adduct $[M + Na]^+$ at 525.0157 and 575.0291 amu. This adduct is also present in the mass spectrum at 255.0408 and 305.5092 amu for ligands **1** and **2**, respectively, and may be a consequence of using sodium formate as calibrant.

Catalysis

The catalytic performance of ruthenium(II) complexes **5–8** was evaluated in the reduction of nitroarenes in the presence of

Table 1 Screening of complexes **5–8** in the reduction of nitrobenzene^a

Entry	Catalyst	Time (min)	Yield (%)
1	—	30	1
2	5	30	>99
3	6	30	97
4	7	30	95
5	8	30	90
6	—	60	1
7	$[RuCl_2(p\text{-cymene})]_2$	60	13
8	5	60	100
9	6	60	100
10	7	60	100
11	8	60	100
12	5	30	>99 ^b
13	5	30	90 ^c

^a Reaction conditions: nitrobenzene (0.3 mmol), $NaBH_4$ (1.2 mmol), ethanol (2 mL), room temperature. Yields were determined by GC-MS.

^b Mercury drop test. ^c Catalyst charge of 0.5, 10% of azobenzene was also detected.

$NaBH_4$, with nitrobenzene as the model substrate. As shown in Table 1, all complexes were very active in the reduction of nitrobenzene to aniline with excellent yields in the range of 90–99% in 30 min (Table 1, entries 2–5). No reaction was observed in the control experiment performed without the ruthenium catalyst (Table 1, entries 1 and 6). The use of $[RuCl_2(p\text{-cymene})]_2$ as catalyst afforded the expected product in 13% yield (Table 1, entry 7). Moreover, the homogeneity of the catalytic reaction was tested using the mercury drop experiment in the reduction of nitrobenzene with catalyst **5**, which gave a >99% of aniline as the product with no loss of efficiency (Table 1, entry 12). On the other hand, decreasing the catalyst loading to 0.5% mol gave 90% yield of aniline with the formation of 10% of azobenzene (Table 1, entry 13 and Fig. S114–S116†).

As shown in Table 1, no significant differences in the catalytic activity of complexes **5–8** can be observed, especially at 60 min (Table 1, entries 8–11). Therefore, another model substrate (4-aminonitrobenzene) was evaluated (Table S6†). Furthermore, to better assess the role of the heterocyclic moiety on catalysis, complexes **10** (synthesized from triazene **9**) and **11**^{13d} were introduced as controls for catalysts **5–8**, in which the heterocyclic moiety was replaced in the structure of complexes by a phenyl or *p*-tolyl fragment (Chart 2).

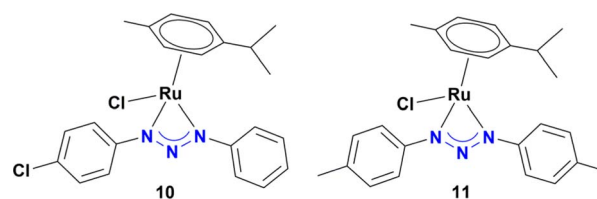


Chart 2 Ru(II) complexes used as controls.



We expanded the scope of the catalytic reduction to a series of nitroarenes using **5** as the catalyst (1% mol), at room temperature in the presence of four equivalents of NaBH₄. As shown in Table 2, catalyst **5** is found to be very active in the reduction of a diverse group of nitroarenes. Electron-withdrawing and electron-donating substituents on the aromatic ring provided the expected products in good to excellent yields (Table 2, 78–100%).

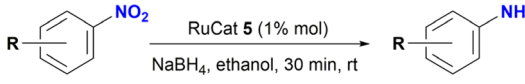
The reduction of the NO₂ group in the presence of other functionality groups such as –OH, –COOEt and –CONHR was also explored. In the case of the aldehyde group, the carbonyl was reduced along with the NO₂ group, as observed in other Ru(II) *p*-cymene catalytic systems (Table 2, entries 3–6).^{12f–k}

The degree of substitution pattern on the aromatic ring had no effect on catalytic efficiency. For example, compound **5** was able to reduce the nitro group in the presence of aldehyde and methoxy groups, with the aldehyde also being reduced to the alcohol with 100% yield (Table 2, entries 6–8). In this case, reduction of the aldehyde is attributed to the NaBH₄ itself, which was used in excess. Noteworthy, the presence of a hydroxyl group in *para*-position to the –NO₂, led to the same conversion of the expected amine (~80% *ca.*), regardless of the presence of other functional groups or degree of substitution (entries 2 and 9–10, Table 2). In contrast, the reduction of the (4-nitrophenyl)methanol proceeded smoothly with a 100% yield (Table 2, entry 3).^{12f,19}

1-Iodo-4-nitrobenzene was readily reduced to 4-iodoaniline in 30 minutes with quantitative yield (Table 2, entry 4).^{12c,20a,b} On the other hand, the reaction towards the 2,6-diiodo-4-nitroaniline was not chemoselective, since a mixture of the dehydrohalogenated aniline and the desired product was obtained (Table 2, entry 5 and Fig. S146†). Longer reaction time increased the conversion to the mono iodo-diaminobenzene (63%), while decreasing the yield of the desired 2,6-diiodobenzene-1,4-diamine (35%). For analogous derivatives, a similar behaviour was observed because the hydrogenolysis of the carbon–halogen bond is enhanced by amino substitution in the aromatic ring.^{20c}

The reduction of nitroarenes in the presence of ester, amide and cyano groups was also performed. For example, ethyl-4-nitrobenzoate¶ afforded the product 4-amino-benzyl-alcohol with 57% yield (Table 2, entry 11), the remaining 43% corresponds to the reduction of only the ester group, with the –NO₂ remaining unaffected (Fig. S157–S159†). In this instance both functional groups are reduced, contrary to the behaviour reported in a previous work.^{12d} Furthermore, in another related Ru(II) system^{12b} only the –NO₂ group is reduced, in the 4-nitrobenzoyl chloride substrate. On the other hand, the reduction of *N*-hexyl-4-nitrobenzamide|| is chemoselective towards the nitro group, yielding the expected aniline with 97% conversion (Table 2, entry 12 and Fig. S160–S162†). For multiple bond substituted substrates, like 4-nitrobenzonitrile, the reduction did not

Table 2 Screening of substrates for reduction of nitroarenes catalysed by **5**^a

			
Entry	Substrate	Product	Yield (%)
1			100
2			78
3			100
4			100
5			78/22
6			100
7			100
8			100
9			79 ^b
10			80 ^b
11			43/57 ^c
12			97
13			97
14			8/30

^a Reaction conditions: nitroarene (0.3 mmol), catalyst **5** (0.003 mmol), NaBH₄ (1.2 mmol), ethanol (2 mL) room temperature. Yields were determined by GC-MS. ^b Isolated yield, ¹H NMR of products can be found in ESI. ^c 95% reduction to 4-aminobenzyl alcohol was completed after 120 min.

¶ Ethyl-4-nitrobenzoate (Table 2, entry 11) was generated *in situ* from the reaction of *p*-nitrobenzoyl chloride with ethanol.

|| *N*-Hexyl-4-nitrobenzamide (Table 2, entry 12) was generated *in situ* from the reaction of *p*-nitrobenzoyl chloride with hexylamine.



proceed as expected with only 8% conversion to the corresponding aromatic amine (Table 2, entry 14). Furthermore, the partial hydrogenation of the nitrile bond to imine ensued (30%), with no concomitant reduction of the nitro group, and starting substrate (62%, Fig. S166–S169†).

Unlike the behaviour seen for the ester group (*vide supra*), longer reaction times resulted in additional products observed by GC-MS, including the formation of the amide derivative, but as previously observed without the reduction of the nitro group (Fig. S170†). Finally, the nitro group of 4-(2-fluoro-4-nitrophenyl)morpholine, an important pharmaceutical intermediate for the synthesis of the antibiotic Linezolid, was reduced with 97% yield (Table 2, entry 13 and Fig. S163†).

Mechanism insights studies

To determine a plausible mechanism for the reduction of nitroarenes, and ascertain the active species, several experiments were performed. Previous work showed that ruthenium metal hydrides behave as active species in the reduction of nitroarenes under homogeneous catalytic conditions.^{12a–c,f} Therefore, the formation of hydrides was explored in alcohols with and without NaBH₄, as well as in the presence of KOH. For instance, we found that an orange solution of **5** in methanol changed its color, slowly over time (~48 h), to give a red-dark solution, which was analysed by ¹H NMR. Interestingly, no traces of hydrides were detected; instead, a new organometallic species was found (**12**), which was formulated as the coordination isomer of **5** (Scheme 3). Furthermore, complex **6** dissolved in methanol behaves as **5**, giving the coordination isomer **13** (Scheme 3).

Compounds **12** and **13** were fully characterized by NMR, MS and X-ray diffraction analysis. The crystalline structure of both complexes shows the coordination of the heterocyclic moiety to give a five-membered chelate where the central nitrogen of the triazenide system coordinates to the ruthenium metal ion (Fig. 4 and S98†).

On the other hand, addition of four equivalents of NaBH₄ to a solution of **5** in methanol-*d*₄ gave a mixture of four organometallic species along unreacted complex **5** (ratio 52, 17, 15, 4,

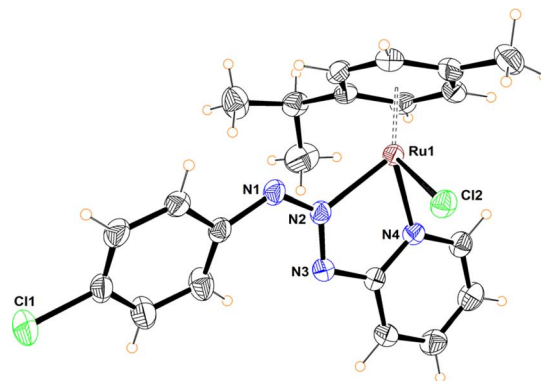
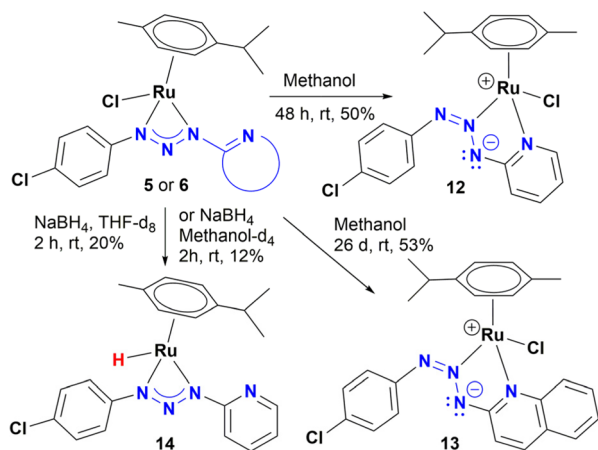


Fig. 4 Molecular structure of complex **12**. Selected bond distances (Å): N(1)–N(2), 1.285(4); N(2)–N(3), 1.337(3); Ru(1)–N(2), 2.062(3); Ru(1)–N(4), 2.060(2); Ru(1)–Cl(2), 2.4063(8). Selected bond angles (°): N(2)–Ru(1)–N(4), 75.8(1); N(2)–Ru(1)–Cl(2), 83.97(7); N(4)–Ru(1)–Cl(2), 84.56(7). N(2)–N(3)–N(4), 122.3(2).

and 12%). Two of them were identified as Ru-hydrides with NMR signals at –3.04 and –5.64 ppm (Fig. S177–S178†). The NMR data of the most abundant Ru-hydride (–3.04 ppm) is consistent with the proposed structure (**14**) shown in Scheme 3, being the least abundant Ru-hydride a coordination isomer of **14**. In contrast, if the reaction is carried out in THF-*d*₈, only one Ru-hydride (NMR signal at –2.91 ppm, Fig. S179†) is observed together with the unreacted complex **5** (ratio of 20 to 80%, respectively). Another control experiment carried out in ethanol and KOH (10%) showed that **5** did not catalyse the reduction of nitrotoluene (Table S7†). Moreover, the equimolar reaction of **5** in either methanol, ethanol or 2-propanol did not yield **14**. Based on these experiments, the mechanism shown in Scheme 4 is proposed. The catalytic cycle may include participation of the hydride **14**, which has been previously synthesized and detected by NMR (Scheme 4). Thus, coordination of nitrobenzene gives species **A**, possibly by decooordination of one nitrogen of the triazenide ligand, which has proven to be a labile ligand in the isomerization of **5** to **12** in alcohols. Then, species **A** could transform into **B** by a hydride migration to nitrogen. This is a reaction that is probably assisted by the movement of a pair of electrons of the nitroarene as well as hydrogen donation from the solvent. Finally, elimination of water will release nitrosobenzene and allow species **B** to react with NaBH₄ to give **14**.

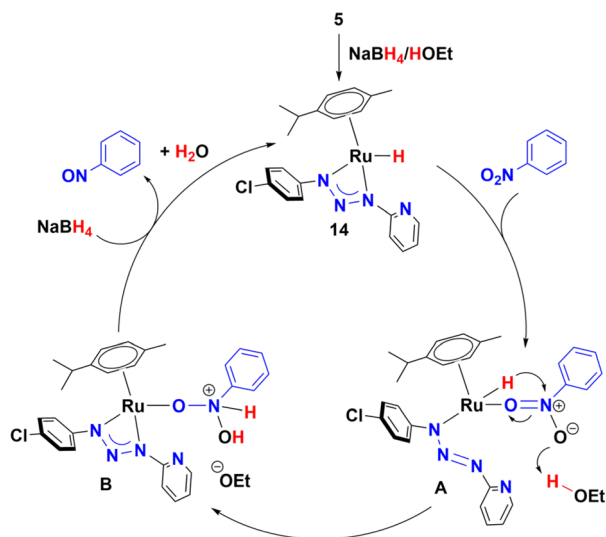
Nitrosobenzene could be hydrogenated in a similar way to give *N*-phenylhydroxylamine, both compounds have been proposed as potential intermediates in a condensation mechanism proposed by Haber.^{4b} As noted in Table 1 (entry 13), azobenzene was detected by GC-MS under catalytic conditions (Fig. S112 and S114†). Therefore, azobenzene and azoxybenzene** could be the products of the condensation of nitrosobenzene and *N*-phenylhydroxylamine, which is consistent with a Haber mechanism (Scheme 5).

** Azoxybenzene was not detected. However, their analogues azoxytoluene and azotoluene were detected in the reduction of nitrotoluene (Fig. S171 and S174†).

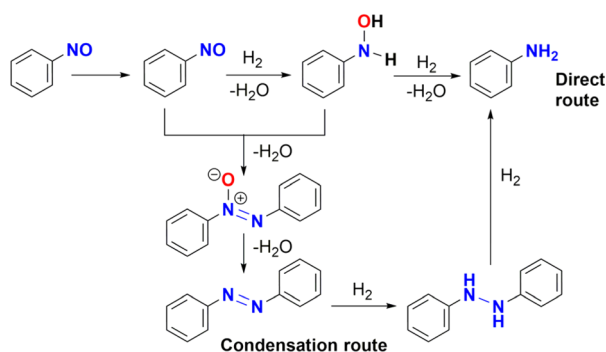


Scheme 3 Exploration of ruthenium hydride formation.





Scheme 4 Proposed mechanism for reduction of nitrobenzene.



Scheme 5 Haber mechanism for hydrogenation of nitrobenzene.

Finally, the reutilization of the catalytic system was tested by addition of more substrate once the catalysis was completed in the first run (>99% yield, using 4-nitrotoluene as substrate). After the second addition of 4-nitrotoluene, no hydrogenation ensued, while the subsequent incorporation of four equivalents of NaBH_4 to the reaction mixture resulted in >99% yield; one additional run afforded the same result (Chart S1†). These results mean that the catalytic system requires the subsequent addition of NaBH_4 in order to be active, and can be reutilized up to three times.

In summary, the use of polar solvents like methanol or ethanol favours the isomerization of complexes 5 and 6 to their coordination isomers 12 and 13, respectively. Moreover, the addition of NaBH_4 is crucial for both, catalysis and the formation of the Ru-hydride 14. Interestingly, under the same catalysis conditions the coordination isomer 12 was as effective as 5, giving the hydrogenation product of nitrobenzene with >99% yield.

Conclusions

Four air-stable and easily handled Ru(II) complexes of triazenide ligands bearing different heterocyclic moieties were prepared

and fully characterized by spectroscopic and spectrometric techniques. In complex 7, ligand 3 coordinates to the metal through the central nitrogen of the triazenide system and the nitrogen of the imidazole forming a five-membered chelate ring. In compounds 5, 6, and 8 a bidentate four-membered chelate ring was obtained where the ligand coordinates through the terminal nitrogen atoms of the triazenide system regardless of the heterocyclic moiety. However, a change in the coordination mode of the triazenide ligand is observed when complexes 5 and 6 were dissolved in alcohols giving the coordination isomers 12 and 13. In these complexes the triazenide ligand coordinates to the metal ion through the central nitrogen and the heterocyclic moiety forming a five-membered chelate. The molecular structures of complexes 5, 6, 7, 12, and 13 were confirmed by X-ray diffraction analysis. Complexes 5–8 were tested in the catalytic reduction of nitroarenes. All complexes were found to be highly active in the reduction of nitrobenzene to aniline. Moreover, complex 5 bearing a pyridine ring, displayed the best catalytic performance with structurally diverse substrates and a wide functional group tolerance to afford the desired aromatic amines in good to excellent yields under mild conditions. The introduction of an N-heterocycle in the structure of the ligand seems to improve the catalytic activity of the complexes, since higher yields of products can be obtained compared to the tested controls. Studies are underway to further extend the scope of substrates and to the use of greener methodologies.

Experimental

Materials and methods

Unless otherwise specified, all manipulations were carried out in an argon-filled glovebox or using Schlenk techniques. Commercially available reagents were used as received from Aldrich Chemical Co. and Alfa Aesar. $[\text{RuCl}_2(p\text{-cymene})]_2$ was prepared by published procedures;²¹ 1-[(4-methyl)phenyl]-3-[(4-*tert*-butyl-2-methyl)imidazole-1-yl]triazene (3), 1-[(4-methyl)phenyl]-3-[(2-methyl)imidazole-1-yl]triazene (4), and $[\text{Ru}\{1,3\text{-bis}(4'\text{-methyl phenyl})\text{triazene}\}(\text{Cl})(p\text{-cymene})]$ (11) were previously synthesized by our group.^{13b,d} The preparation and characterization of $[\text{RuCl}(\text{ClPh-triazene-Ph})(p\text{-cymene})]$ (10) is given in the experimental and ESI.† DMSO- d_6 , $(\text{CD}_3)_2\text{CO}$, CDCl_3 and CD_2Cl_2 were used as received from CIL. NMR spectra were recorded at 400 MHz with Bruker Avance III spectrometer at 30 °C unless otherwise specified. ^1H and ^{13}C NMR chemical shifts are reported in ppm referenced to residual solvent resonances (^1H NMR: 7.24 for CHCl_3 in CDCl_3 , 5.32 for CHDCl_2 in CD_2Cl_2 , 2.50 for DMSO in DMSO- d_6 , 2.05 for acetone- d_6 in acetone- d_6 ; ^{13}C $\{^1\text{H}\}$ NMR: 77.23, 54.0, 39.51 and 29.92 for CDCl_3 , CD_2Cl_2 , DMSO- d_6 , and acetone- d_6 , respectively). Coupling constants J are given in Hertz (Hz). FT-IR spectra were recorded on a PerkinElmer FT-IR 1605 spectrophotometer (ATR mode). Melting points were measured in an Electrothermal GAC 88629 apparatus. Mass spectra were obtained by direct insertion on an Agilent Technologies 5975C instrument. High Resolution Mass Spectrometry (HRMS) data were obtained in a micrOTOF-Q III MS instrument with electrospray ionization using sodium



formate as calibrant. A complete set of NMR and HRMS spectra has been provided in the ESI,[†] as evidence of bulk purity and identity. X-ray diffraction data for crystals of compounds **5**, **6**, **7**, **12**, and **13** were collected on an Agilent Technologies Supernova AtlasS2 and a Bruker APEX II CCD diffractometers.

Synthetic procedures

1-(2'-Pyridyl)-3-(4'-chlorophenyl)triazene (1). In a 300 mL round bottom flask, *p*-chloro-aniline (2.55 g, 20 mmol) was suspended at -4°C , in a 10% aqueous solution of HCl (18.5 mL, 60 mmol), and stirred for 35 min. A 15% cold solution of NaNO_2 (12 mL, 26 mmol) was added drop wise, along with a cold aqueous solution of 2-amine-pyridine (1.91 g, 20 mmol) and stirred for 8 h. The reaction mixture was neutralized with NaHCO_3 (5.05 g, 60 mmol) and stirred for additional 2 h. The resulting precipitated was filtered and dried *in vacuo* to afford a pale yellow solid (3.38 g, 73%). M. P. $178\text{--}184^{\circ}\text{C}$. ^1H NMR (400.1 MHz, CDCl_3): δ 11.51 (br s, 1H, NH), 8.43 (br d, $^3J_{\text{HH}} = 4.0$ Hz, 1H, H6-Py), 7.69 (ddd, $^3J_{\text{HH}} = 8.4$, $^3J_{\text{HH}} = 7.3$ Hz, $^4J_{\text{HH}} = 1.8$ Hz, 1H, H5-Py), 7.57–7.52 (m, 3H, 2H-Ar, H4-Py), 7.37 (d, $^3J_{\text{HH}} = 8.4$ Hz, 2H, Ar), 6.99 (dd, $^3J_{\text{HH}} = 6.0$, $^3J_{\text{HH}} = 6.0$ Hz, 1H, H3-Py) ppm. ^{13}C $\{^1\text{H}\}$ NMR (100.6 MHz, CDCl_3): δ 154.7 (C2, Py), 148.2 (C6, Py), 148.2 (C1, Ar), 138.7 (C4, Py), 133.6 (C4, Ar), 129.5 (2C, Ar), 123.0 (2C, Ar), 118.6 (C5, Py), 109.0 (C3, Py) ppm. MS (70 eV) m/z (%): $[\text{M}]^+$ 232 (16), $[\text{M}-\text{NH}(\text{C}_5\text{H}_4\text{N})]^+$ 139 (80), $[\text{M}-\text{N}_3\text{H}(\text{C}_5\text{H}_4\text{N})]^+$ 111 (100). HRMS (ESI-TOF) m/z : $[\text{M} + \text{Na}]^+$ calcd for $\text{C}_{11}\text{H}_9\text{ClN}_4\text{Na}$ 255.0401; found 255.0408. FT-IR (ATR, cm^{-1}): 3169 $\nu(\text{N}-\text{H})$, 3094, 2960, 2780, 1598, 1532, 1198, 1088, 994, 830, 764.

1-(2'-Quinoly)-3-(4'-chlorophenyl)triazene (2). At room temperature in a 250 mL round bottom flask, *p*-chloro-aniline was suspended in a 10% solution of HCl (6.4 mL, 20.8 mmol) and stirred for 10 min. The temperature of the solution was lowered to -4°C in an ice-bath; a 15% cold solution of NaNO_2 (6.3 mL, 9.02 mmol) was added dropwise and stirred for 1 h. A cold solution of 2-amine-quinoline (1000 mg, 6.94 mmol, dissolved in 40 mL of distilled water and 10 mL of MeOH), was added to the reaction mixture and stirred at -4°C for 8 h. The solution was neutralized with NaHCO_3 (1.75 g, 20.8 mmol) and stirred for 1 h. The resulting precipitated was filtered and dried under vacuum to afford a pale yellow solid (1.46 g, 75%). M. P. = $202\text{--}206^{\circ}\text{C}$. ^1H NMR (400.1 MHz, $\text{DMSO}-d_6$): δ 13.12 (br s, 1H, NH), 8.34 (d, $^3J_{\text{HH}} = 8.8$ Hz, 1H, H4-Qui), 7.91 (br d, $^3J_{\text{HH}} = 7.2$ Hz, 1H, H5-Qui), 7.81 (d, $^3J_{\text{HH}} = 8.4$ Hz, 1H, H8-Qui), 7.79 (d, $^3J_{\text{HH}} = 8.4$ Hz, 1H, H3-Qui), 7.70 (ddd, $^3J_{\text{HH}} = 8.4$, $^3J_{\text{HH}} = 6.8$, $^4J_{\text{HH}} = 1.6$ Hz, 1H, H7-Qui), 7.63 (d, $^3J_{\text{HH}} = 8.0$ Hz, 2H, H3-Ar), 7.52 (d, $^3J_{\text{HH}} = 8.0$ Hz, 2H, H2-Ar), 7.45 (ddd, $^3J_{\text{HH}} = 8.0$, $^3J_{\text{HH}} = 6.8$, $^4J_{\text{HH}} = 1.2$ Hz, 1H, H6-Qui) ppm. ^{13}C $\{^1\text{H}\}$ NMR (100.6 MHz, $\text{DMSO}-d_6$): δ 153.9 (C2, Qui), 147.8 (C1, Ar), 146.6 (C8a, Qui), 138.6 (C4, Qui), 131.6 (C4, Ar), 130.1 (C7, Qui), 129.2 (C3, Ar), 128.0 (C5, Qui), 126.8 (C8, Qui), 125.4 (C4a, Qui), 124.4 (C6, Qui), 122.5 (C2, Ar), 110.5 (C3, Qui) ppm. HRMS (ESI-TOF) m/z : $[\text{M} + \text{Na}]^+$ calcd for $\text{C}_{15}\text{H}_{11}\text{ClN}_4\text{Na}$ 305.0564; found 305.0562. FT-IR (ATR, cm^{-1}): 3185 $\nu(\text{N}-\text{H})$, 3056, 3026, 1602, 1572, 1504, 1429, 1188, 1085, 825, 751, 691.

[RuCl $\{1-(2'\text{-py})-3-(4'\text{-ClPh})\text{triazenide}\}(p\text{-cymene})\}$ (5). A mixture of **1** (200.2 mg, 0.859 mmol) and Et_3N (0.48 mL, 3.44

mmol) in 9 mL of CH_3CN , was stirred for 30 min. $[\text{RuCl}_2(p\text{-cymene})]_2$ (263.1 mg, 0.429 mmol) was added to the reaction mixture and stirred for 24 h. The resulting brown-orange suspension was filtered to remove the orange solid, which was washed with water (3×15 mL) and dried under vacuum to afford the product as an orange microcrystalline solid (251.3 mg, 58%). X-ray quality crystals were obtained by vapour diffusion of pentane to a concentrated solution of **5**. M. P. $234\text{--}238^{\circ}\text{C}$. ^1H NMR (400.1 MHz, CDCl_3): δ 8.43 (d, $^3J_{\text{HH}} = 4$ Hz, 1H, H6-Py), 7.55 (dd, $^3J_{\text{HH}} = 7.6$ Hz, $^3J_{\text{HH}} = 7.2$ Hz, 1H, H4-Py), 7.43 (d, $^3J_{\text{HH}} = 8$ Hz, 1H, H3-Py), 7.35–7.28 (m, 4H, Ar), 6.97 (dd, $^3J_{\text{HH}} = 5.6$ Hz, $^3J_{\text{HH}} = 6$ Hz, 1H, H5-Py), 6.07 (d, $^3J_{\text{HH}} = 5.6$ Hz, 1H, Ar, *p*-cymene), 5.81 (d, $^3J_{\text{HH}} = 5.6$ Hz, 1H, Ar, *p*-cymene), 5.53 (d, $^3J_{\text{HH}} = 6.0$ Hz, 1H, Ar, *p*-cymene), 5.48 (d, $^3J_{\text{HH}} = 6.0$ Hz, 1H, Ar, *p*-cymene) 2.88 [sept, $^3J_{\text{HH}} = 6.8$ Hz, $\text{CH}(\text{CH}_3)_2$, *p*-cymene], 2.32 (s, 3H, CH_3 , *p*-cymene), 1.26 [d, $^3J_{\text{HH}} = 6.4$ Hz, 3H, $\text{CH}(\text{CH}_3)_2$, *p*-cymene], 1.25 ppm [d, $^3J_{\text{HH}} = 6.8$ Hz, 3H, $\text{CH}(\text{CH}_3)_2$, *p*-cymene]. ^{13}C $\{^1\text{H}\}$ NMR (100.6 MHz, CDCl_3): δ 158.9 (C2, Py), 149.1 (C6, Py), 145.5 (C1, Ar), 137.0 (C4, Py), 130.5 (C4, Ar), 129.1 (2C, Ar), 119.5 (C5, Py), 119.0 (2C, Ar), 109.7 (C3, Py), 103.1 (C-*i*Pr, *p*-cymene), 101.6 (C- CH_3 , *p*-cymene), 83.1 (CH, Ar, *p*-cymene), 81.0 (CH, Ar, *p*-cymene), 80.5 (CH, Ar, *p*-cymene), 79.8 (CH, Ar, *p*-cymene), 31.9 [$\text{CH}(\text{CH}_3)_2$, *p*-cymene], 22.9 [$\text{CH}(\text{CH}_3)_2$, *p*-cymene], 22.7 [$\text{CH}(\text{CH}_3)_2$, *p*-cymene], 19.5 (CH_3 , *p*-cymene) ppm. ^1H NMR (400.1 MHz, $\text{THF}-d_8$): δ 8.36 (d, $^3J_{\text{HH}} = 4$ Hz, 1H, H6-Py), 7.53 (t, $^3J_{\text{HH}} = 8.0$ Hz, 1H, H4-Py), 7.39–7.34 (m, 3H, 2H-Ar, H3-Py), 7.27 (d, $J = 8.8$ Hz, 2H, Ar), 6.94 (t, $^3J_{\text{HH}} = 8.0$ Hz, 1H, H5-Py), 6.07 (d, $^3J_{\text{HH}} = 5.8$ Hz, 1H, Ar, *p*-cymene), 5.91 (d, $^3J_{\text{HH}} = 5.8$ Hz, 1H, Ar, *p*-cymene), 5.54 (dd, $^3J_{\text{HH}} = 8.7$ Hz, $^3J_{\text{HH}} = 6.2$ Hz, 2H, Ar, *p*-cymene), 2.88 [sept, $^3J_{\text{HH}} = 6.9$ Hz, $\text{CH}(\text{CH}_3)_2$, *p*-cymene], 2.24 (s, 3H, CH_3 , *p*-cymene), 1.23 [dd, $^3J_{\text{HH}} = 6.9$ Hz, 6H, $\text{CH}(\text{CH}_3)_2$, *p*-cymene]. ^{13}C $\{^1\text{H}\}$ NMR (100.6 MHz, $\text{THF}-d_8$): δ 160.59 (C2, Py), 149.6 (C6, Py), 147.1 (C1, Ar), 137.4 (C4, Py), 130.5 (C4, Ar), 129.5 (2C, Ar), 120.0 (C5, Py), 119.9 (2C, Ar), 110.0 (C3, Py), 103.9 (C-*i*Pr, *p*-cymene), 101.9 (C- CH_3 , *p*-cymene), 84.0 (CH, Ar, *p*-cymene), 81.7 (CH, Ar, *p*-cymene), 81.3 (CH, Ar, *p*-cymene), 80.3 (CH, Ar, *p*-cymene), 32.8 [$\text{CH}(\text{CH}_3)_2$, *p*-cymene], 23.1 [$\text{CH}(\text{CH}_3)_2$, *p*-cymene], 22.9 [$\text{CH}(\text{CH}_3)_2$, *p*-cymene], 19.5 (CH_3 , *p*-cymene) ppm. ^1H NMR (400.1 MHz, methanol- d_4): δ 8.35 (ddd, $^3J_{\text{HH}} = 5$ Hz, $^4J_{\text{HH}} = 1.9$ Hz, $^5J_{\text{HH}} = 0.9$ Hz, 1H, H6-Py), 7.70 (ddd, $^3J_{\text{HH}} = 7.8$ Hz, $^4J_{\text{HH}} = 1.7$ Hz, 1H, H4-Py), 7.31–7.44 (m, 5H, Ar, H3), 7.07 (ddd, $^3J_{\text{HH}} = 6.1$ Hz, $^4J_{\text{HH}} = 1.0$ Hz, 1H, H5-Py), 6.13 (d, $^3J_{\text{HH}} = 5.8$ Hz, 1H, Ar, *p*-cymene), 6.03 (d, $^3J_{\text{HH}} = 5.8$ Hz, 1H, Ar, *p*-cymene), 5.64 (d, $^3J_{\text{HH}} = 6.0$ Hz, 1H, Ar, *p*-cymene), 5.62 (d, $^3J_{\text{HH}} = 6.0$ Hz, 1H, Ar, *p*-cymene) 2.78 [sept, $^3J_{\text{HH}} = 6.9$ Hz, $\text{CH}(\text{CH}_3)_2$, *p*-cymene], 2.27 (s, 3H, CH_3 , *p*-cymene), 1.227 [d, $^3J_{\text{HH}} = 6.9$ Hz, 3H, $\text{CH}(\text{CH}_3)_2$, *p*-cymene], 1.224 ppm [d, $^3J_{\text{HH}} = 6.9$ Hz, 3H, $\text{CH}(\text{CH}_3)_2$, *p*-cymene] ppm. HRMS (ESI-TOF) m/z : $[\text{M} + \text{H}]^+$ calcd for $\text{C}_{21}\text{H}_{23}\text{Cl}_2\text{N}_4\text{Ru}$ 503.0337; found 503.0327.

[RuCl $\{1-(2'\text{-qui})-3-(4'\text{-chlorophenyl})\text{triazenide}\}(p\text{-cymene})\}$ (6). Compound **6** was synthesized in a similar manner as complex **5**, using triazene **2** 150.0 mg, 0.530 mmol, Et_3N (215 μL , 2.12 mmol) and $[\text{RuCl}_2(p\text{-cymene})]_2$ (162.4 mg, 0.265 mmol), to yield a microcrystalline orange solid (148.1 mg, 51%); M. P. $186\text{--}190^{\circ}\text{C}$. ^1H NMR (400.1 MHz, CD_2Cl_2): δ 8.02 (d, $^3J_{\text{HH}} = 8.8$ Hz, 1H, H4-Qui), 7.99 (d, $^3J_{\text{HH}} = 8.4$ Hz, 1H, H8-Qui), 7.78 (dd, $^3J_{\text{HH}}$



= 8.0, $^4J_{\text{HH}} = 1.2$ Hz, 1H, H5-Qui), 7.71 (d, $^3J_{\text{HH}} = 9.2$ Hz, 1H, H3-Qui), 7.69 (ddd, $^3J_{\text{HH}} = 8.4$, $^3J_{\text{HH}} = 8.4$, $^4J_{\text{HH}} = 1.6$ Hz, 1H, H7-Qui), 7.44 (ddd, $^3J_{\text{HH}} = 8.0$, $^3J_{\text{HH}} = 8.0$, $^4J_{\text{HH}} = 0.8$ Hz, 1H, H6-Qui), 7.40–7.33 (m, 4H, Ar), 6.16 (d, $^3J_{\text{HH}} = 6.0$ Hz, 1H, Ar, *p*-cymene), 5.89 (d, $^3J_{\text{HH}} = 5.6$ Hz, 1H, Ar, *p*-cymene), 5.65 (d, $^3J_{\text{HH}} = 6.0$ Hz, 1H, Ar, *p*-cymene), 5.56 (d, $^3J_{\text{HH}} = 6.0$ Hz, 1H, Ar, *p*-cymene), 2.90 [sept, $^3J_{\text{HH}} = 7.2$ Hz, 1H, CH(CH₃)₂, *p*-cymene], 2.32 (s, 3H, CH₃, *p*-cymene), 1.25 [d, $^3J_{\text{HH}} = 6.8$ Hz, 3H, CH(CH₃)₂, *p*-cymene], 1.24 [d, $^3J_{\text{HH}} = 6.8$ Hz, 3H, CH(CH₃)₂, *p*-cymene] ppm. ^{13}C { ^1H } NMR (100.6 MHz, CD₂Cl₂): δ = 158.4 (C2, Qui), 148.5 (C8a, Qui), 145.9 (C1, Ar), 137.4 (C4, Qui), 131.1 (C4, Ar), 130.0 (C7, Qui), 130.2 (C3, Ar), 128.8 (C8, Qui), 128.1 (C6, Qui), 127.0 (C4a, Qui), 125.3 (C6, Qui), 119.5 (C2, Ar), 109.9 (C3, Qui), 103.7 (C-*i*Pr, *p*-cymene), 101.7 (C-CH₃, *p*-cymene), 83.6 (CH, Ar, *p*-cymene), 81.4 (CH, Ar, *p*-cymene), 81.2 (CH, Ar, *p*-cymene), 80.3 (CH, Ar, *p*-cymene), 32.3 [CH(CH₃)₂, *p*-cymene], 23.0 [CH(CH₃)₂, *p*-cymene], 22.8 [CH(CH₃)₂, *p*-cymene], 19.7 (CH₃, *p*-cymene) ppm. ^1H NMR (400.1 MHz, DMSO-*d*₆): δ 8.20 (d, $^3J_{\text{HH}} = 8.9$ Hz, 1H, H4-Qui), 7.98 (d, $^3J_{\text{HH}} = 8.4$ Hz, 1H, H8-Qui), 7.87 (d, $^3J_{\text{HH}} = 7.2$ Hz, 1H, H5-Qui), 7.74 (dd, $^3J_{\text{HH}} = 8.3$, 6.2 Hz, 1H, H7-Qui), 7.66 (d, $^3J_{\text{HH}} = 8.9$ Hz, 1H, H3-Qui), 7.50–7.39 (m, 5H, CH-Ar and H7-Qui), 6.23 (d, $^3J_{\text{HH}} = 6.0$ Hz, 1H, Ar, *p*-cymene), 6.19 (d, $^3J_{\text{HH}} = 6.0$ Hz, 1H, Ar, *p*-cymene), 5.86 (d, $^3J_{\text{HH}} = 6.0$ Hz, 1H, Ar, *p*-cymene), 5.83 (d, $^3J_{\text{HH}} = 6.0$ Hz, 1H, Ar, *p*-cymene), 2.83 [sept, $^3J_{\text{HH}} = 6.8$ Hz, 1H, CH(CH₃)₂, *p*-cymene], 2.22 (s, 3H, CH₃, *p*-cymene), 1.20 [d, $J = 6.9$ Hz, 3H, CH(CH₃)₂, *p*-cymene], 1.18 [d, $J = 6.9$ Hz, 3H, CH(CH₃)₂, *p*-cymene] ppm. ^{13}C { ^1H } NMR (100.6 MHz, DMSO-*d*₆): δ 157.2 (C2, Qui), 147.3 (C8a, Qui), 145.0 (C1, Ar), 137.1 (C4, Qui), 129.8 (C4, Ar), 129.2 (C7, Qui), 128.8 (C3, Ar), 128.0 (C8, Qui), 127.7 (C5, Qui), 125.8 (C4a, Qui), 124.8 (C6, Qui), 119.2 (C2, Qui), 109.5 (C3, Qui), 101.9 (C-*i*Pr, *p*-cymene), 100.2 (C-CH₃, *p*-cymene), 83.1 (CH, Ar, *p*-cymene), 80.9 (CH, Ar, *p*-cymene), 80.4 (CH, Ar, *p*-cymene), 79.6 (CH, Ar, *p*-cymene), 31.1 [CH(CH₃)₂, *p*-cymene], 22.2 [CH(CH₃)₂, *p*-cymene], 22.0 [CH(CH₃)₂, *p*-cymene], 18.9 (CH₃, *p*-cymene) ppm. HRMS (ESI-TOF) *m/z*: [M + Na]⁺ calcd for C₂₅H₂₄Cl₂N₄RuNa 575.0314; found 575.0292.

[RuCl(MePhNNN(Me-Im))(*p*-cymene)] (7). In the glovebox, in a 50 mL round bottom flask fitted with a spin bar, triazene 3 (0.088g, 0.41 mmol), and KN(SiMe₃)₂ (0.082 g, 0.41 mmol) were dissolved in dry THF (5 mL) and stirred for 10 min; [RuCl₂(*p*-cymene)]₂ (0.126 g, 0.21 mmol) was added, and the solution was stirred for an additional 2 h. The reaction mixture was filtered through a Celite plug, and the solvent removed under vacuum, to afford a brown solid (0.18 g, 90%). M. P. 178–182 °C. ^1H NMR (400 MHz, Acetone-*d*₆): δ 7.75 (d, $J = 8.3$ Hz, 2H, Ar), 7.14 (d, $J = 1.8$ Hz, 1H, H4, Im), 7.12 (d, $J = 8.3$ Hz, 2H, Ar), 6.72 (d, $J = 1.8$ Hz, 1H, H5, Im), 5.66 (t, $J = 5.8$ Hz, 2H, Ar, *p*-cymene), 5.38 (m, $J = 5.4$ Hz, 2H, Ar, *p*-cymene), 3.42 (s, 3H, NCH₃), 2.85 (sept, $J = 6.9$ Hz, 1H, CH(CH₃)₂, *p*-cymene), 2.31 (s, 3H, Ar-CH₃), 2.18 (s, 3H, CH₃, *p*-cymene), 1.19 (d, $J = 6.9$ Hz, 6H, CH(CH₃)₂, *p*-cymene). ^{13}C { ^1H } NMR (100.6 MHz, Acetone-*d*₆): δ 161.2 (C2, Im), 149.5 (C1, Ar), 134.8 (C4, Ar), 129.0 (C3, Ar), 125.9 (C4, Im), 125.6 (C2, Ar), 117.6 (C5, Im), 102.2 (C-*i*Pr, *p*-cymene), 100.5 (C-CH₃, *p*-cymene), 87.5 (CH, Ar, *p*-cymene), 86.0 (CH, Ar, *p*-cymene), 84.0 (CH, Ar, *p*-cymene), 83.0 (CH, Ar, *p*-cymene), 33.1 (NCH₃), 31.5 [CH(CH₃)₂, *p*-cymene], 22.5 [CH(CH₃)₂, *p*-cymene],

22.4 [CH(CH₃)₂, *p*-cymene], 21.2 (Ar-CH₃), 18.7 (CH₃, *p*-cymene) ppm. HRMS (ESI-TOF) *m/z*: [M + H]⁺ calcd for C₂₁H₂₇ClN₅Ru 486.0995; found 486.0967.

[RuCl(MePhNNN(Me-*t*Bulm))(*p*-cymene)] (8). Complex 8 was synthesized in a similar manner as complex 7, with the following conditions: 4 (0.1 g, 0.37 mmol), KN(SiMe₃)₂ (0.073 g, 0.37 mmol) and [RuCl₂(*p*-cymene)]₂ (0.121 g, 0.18 mmol) to afford a brown powder (0.17 g, 85%). Slow evaporation from acetone gave X-ray quality crystals. M. P. 148–151 °C. ^1H NMR (400 MHz, Acetone-*d*₆): δ 7.22 (d, $J = 8.3$ Hz, 2H, Ar), 7.10 (d, $J = 8.3$ Hz, 2H, Ar), 6.52 (s, 1H, H5, Im), 6.03 (d, $J = 5.9$ Hz, 1H, Ar, *p*-cymene), 5.97 (d, $J = 5.9$ Hz, 1H, Ar, *p*-cymene), 5.64 (d, $J = 5.9$ Hz, 1H, Ar, *p*-cymene), 5.51 (d, $J = 5.9$ Hz, 1H, Ar, *p*-cymene), 3.52 (s, 3H, NCH₃), 3.08 (sept, $J = 6.9$ Hz, 1H, CH(CH₃)₂, *p*-cymene), 2.29 (s, 3H, Ar-CH₃), 2.28 (s, 3H, CH₃, *p*-cymene), 1.30 [d, 3H, CH(CH₃)₂, *p*-cymene], 1.29 [s, 9H, C(CH₃)₃], 1.28 [d, 3H, CH(CH₃)₂, *p*-cymene] ppm. ^{13}C { ^1H } NMR (100.6 MHz, Acetone-*d*₆): δ 150.0 (C4, Im), 148.1 (C2, Im), 146.0 (C1, Ar), 134.6 (C4, Ar), 130.1 (C3, Ar), 118.2 (C2, Ar), 114.4 (C5, Im), 103.3 (C-*i*Pr, *p*-cymene), 100.7 (C-CH₃, *p*-cymene), 84.9 (Ar-*p*-cymene), 81.7 (Ar-*p*-cymene), 81.3 (Ar-*p*-cymene), 80.9 (Ar, *p*-cymene), 34.8 (NCH₃), 32.5 [C(CH₃)₃], 32.3 [CH(CH₃)₂, *p*-cymene], 30.6 [C(CH₃)₃], 23.1 (Ar-CH₃), 22.7 [CH(CH₃)₂, *p*-cymene], 19.5 (CH₃, *p*-cymene) ppm. HRMS (ESI-TOF) *m/z*: [M + H]⁺ calcd for C₂₅H₃₅ClN₅Ru 542.1622; found 542.1615.

1-(Phenyl)-3-(4'-chlorophenyl)triazene (9). Compound 9 was synthesized in a similar manner as triazene 2, using aniline (365 μL , 4.0 mmol), HCl (3.7 mL, 12 mmol), NaNO₂ (2.4 mL, 5.2 mmol) and *p*-chloroaniline (510.8 mg, 4 mmol) to yield a mustard yellow solid (678.8 mg, 73%). M. P. = 68–70 °C. ^1H NMR (400.1 MHz, DMSO-*d*₆): δ 12.53 (br s, 1H, NH), 7.46–7.40 (m, 8H, Ar), 7.16–7.14 (m, 1H, Ar) ppm. ^{13}C { ^1H } NMR (101 MHz, DMSO): δ 144.7, 129.2, 129.1, 124.68, 119.1, 117.4, 113.1 ppm. ^1H NMR (400 MHz, Acetone-*d*₆): δ 11.42 (s, 1H), 7.51 (t, $J = 7.8$ Hz, 4H), 7.40 (ddd, $J = 11.9$, 7.2, 5.1 Hz, 4H), 7.16 (s, 1H) ppm. MS (70 eV) *m/z* (%): [M]⁺ 231 (12), [M-NH(C₆H₅)]⁺ 139 (66), [M-N₃H(C₆H₅)]⁺ 111 (100). HRMS (ESI-TOF) *m/z*: [M + H]⁺ calcd for C₁₂H₁₁ClN₃ 232.0636; found 232.0630.

[RuCl(ClPh-triazenide-Ph)(*p*-cymene)] (10). 1-[Phenyl]-3-[4'-chlororophenyl]triazene (9) (71.65 mg, 0.3264 mmol, 2.0 eq.) was dissolved in CH₂Cl₂ (5 mL) and triethylamine (66.0 mg, 0.6532 mmol, 4.0 eq.) was added with stirring. Then, a solution of [RuCl₂(*p*-cymene)]₂ (100.0 mg, 0.1632 mmol, 1.0 eq.) in CH₂Cl₂ (5 mL) was slowly added and the mixture stirred for 24 h at room temperature. A dark violet solution was formed, which was filtered through an alumina column. The solvent was removed under reduced pressure to obtain a yellow solid. Recrystallization by vapour diffusion of hexane into a concentrated solution of the product in CH₂Cl₂ at room temperature gave yellow crystals (119.46 mg, 0.23282 mmol, 73%). M. P. = 184–188 °C. ^1H NMR (400 MHz, Acetone-*d*₆): δ 7.42–7.34 (m, 4H), 7.34–7.26 (m, 4H), 7.14–7.04 (m, 1H), 6.15–6.05 (m, 2H), 5.69–5.59 (m, 2H), 2.81 (sept, $J = 6.9$ Hz, 1H), 2.29 (s, 3H), 1.24 (d, $J = 6.9$ Hz, 6H) ppm. ^{13}C { ^1H } NMR (101 MHz, Acetone-*d*₆): δ 146.8, 146.0, 145.8, 129.0, 128.8, 128.8, 128.4, 128.0, 124.5, 118.4, 118.2, 116.9, 103.8, 101.6, 81.9, 78.5, 31.9, 22.1, 18.6 ppm.

HRMS (ESI-TOF) m/z : $[M + Na]^+$ calcd for $C_{22}H_{23}Cl_2N_3RuNa$ 524.0205; found 524.0206.

[RuCH{1-(*N'*-Py)-3-(4'-ClPh)triazenide}(*p*-cymene)] (12). A solution of complex 5 (0.030 g, 0.059 mmol) in 5 mL of methanol was stirred overnight at room temperature, thereupon the colour of the solution changed from light bright orange to dark red; the reaction was stirred for an additional 72 h, dried under vacuum to afford a dark red solid. X-ray quality crystals were obtained by vapour diffusion of hexane to a concentrated solution of 12 in acetone. (0.015 g, 50%). M. P. 1H NMR (400 MHz, THF- d_8): δ 8.65 (d, $^3J_{HH} = 6$ Hz, 1H, H6-Py), 7.64 (d, $^3J_{HH} = 8.9$ Hz, 2H, H3-Ar), 7.41 (ddd, $^3J_{HH} = 8.5, 7.1, 1.6$ Hz, 1H, H4-Py), 7.24 (d, $^3J_{HH} = 8.9$ Hz, 2H, H2-Ar), 6.87 (d, $^3J_{HH} = 8$ Hz, 1H, H3-Py), 6.58 (t, $^3J_{HH} = 5.9$ Hz, 1H, H5-Py), 5.68 (d, $^3J_{HH} = 5.6$ Hz, 1H, Ar, *p*-cymene), 5.64 (d, $^3J_{HH} = 6.0$ Hz, 1H, Ar, *p*-cymene), 5.42 (d, $^3J_{HH} = 6.0$ Hz, 2H, Ar, *p*-cymene), 2.81 [sept, $^3J_{HH} = 6.8$ Hz, CH(CH₃)₂, *p*-cymene], 2.19 (s, 3H, CH₃, *p*-cymene), 1.16 [d, $^3J_{HH} = 6.9$ Hz, 3H, CH(CH₃)₂, *p*-cymene], 1.13 ppm [d, $^3J_{HH} = 6.9$ Hz, 3H, CH(CH₃)₂, *p*-cymene]. ^{13}C { 1H } NMR (100.6 MHz, THF- d_8): δ 168.0 (C2, Py), 151.9 (C6, Py), 150.9 (C1, Ar), 138.2 (C4, Py), 130.2 (C4, Ar), 128.5 (2C, Ar), 115.1 (C5, Py), 126.9.0 (2C, Ar), 114.6 (C3, Py), 103.8 (C-*i*Pr, *p*-cymene), 102.8 (C-CH₃, *p*-cymene), 90.6 (CH, Ar, *p*-cymene), 87.5 (CH, Ar, *p*-cymene), 86.2 (CH, Ar, *p*-cymene, 2C), 31.9 [CH(CH₃)₂, *p*-cymene], 22.8 [CH(CH₃)₂, *p*-cymene], 22.4 [CH(CH₃)₂, *p*-cymene], 18.7 (CH₃, *p*-cymene) ppm.

[RuCH{1-(*N'*-Qui)-3-(4'-ClPh)triazenide}(*p*-cymene)] (13). Compound 13 was synthesized in a similar manner as complex 13, dissolving 6 (0.030 g, 0.054 mmol) in 10 mL of methanol and stirred at room temperature for 26 days, to yield a dark red solid. X-ray quality crystals were obtained by vapour diffusion of hexane to a concentrated solution of 13 in acetone (0.016 g, 53%). 1H NMR (400.1 MHz, CD₂Cl₂): δ 8.24 (d, $^3J_{HH} = 9.0$ Hz, 1H, H8-Qui), 7.83 (d, $^3J_{HH} = 8.8$ Hz, 1H, H4-Qui), 7.70–7.65 (m, 2H, H2-Ar, 2H, H5, H7-Qui), 7.40–7.35 (m, 2H, H3-Ar, 1H, H6-Qui), 7.13 (d, $^3J_{HH} = 8.9$ Hz, 1H, H3-Qui), 5.74 (d, $^3J_{HH} = 5.9$ Hz, 1H, Ar, *p*-cymene), 5.63 (d, $^3J_{HH} = 6.2$ Hz, 1H, Ar, *p*-cymene), 5.49 (t, $^3J_{HH} = 6.2$ Hz, 2H, Ar, *p*-cymene), 2.51 [sept, $^3J_{HH} = 6.9$ Hz, 1H, CH(CH₃)₂, *p*-cymene], 2.33 (s, 3H, CH₃, *p*-cymene), 1.06 [d, $^3J_{HH} = 6.9$ Hz, 3H, CH(CH₃)₂, *p*-cymene], 0.98 [d, $^3J_{HH} = 6.9$ Hz, 3H, CH(CH₃)₂, *p*-cymene] ppm. ^{13}C { 1H } NMR (100.6 MHz, CD₂Cl₂): δ 166.08 (C2, Qui), 149.7 (C1, Ar), 148.5 (C8a, Qui), 137.9 (C4, Qui), 131.3 (C4, Ar), 130.7 (Ar), 128.9 (C3, Ar), 128.7 (C5, Qui), 126.7 (C8, Qui), 126.4 (C7, Qui), 125.2 (C4a, Qui), 124.1 (C6, Qui), 116.1 (C3, Qui), 105.5 (C-CH₃, *p*-cymene), 102.6 (C-*i*Pr, *p*-cymene), 91.3 (CH, Ar, *p*-cymene), 86.9 (CH, Ar, *p*-cymene), 86.6 (CH, Ar, *p*-cymene), 85.1 (CH, Ar, *p*-cymene), 31.5 [CH(CH₃)₂, *p*-cymene], 22.7 [CH(CH₃)₂, *p*-cymene], 22.2 [CH(CH₃)₂, *p*-cymene], 19.3 (CH₃, *p*-cymene) ppm.

[RuH{1-(*N'*-Py)-3-(4'-ClPh)triazenide}(*p*-cymene)] (14). Compound 5 (0.0080 g, 0.0159 mmol) was transferred into a J. Young NMR tube and dissolved in 0.6 mL of THF- d_8 . The resulting orange solution was treated with NaBH₄ (2.9 mg, ~0.063 mmol) to give an orange slightly brown solution. Analysis by NMR showed starting material (~80%) and the Ru-hydride 14 in a ratio of ~20% after 2 h of reaction. 1H NMR (400.1 MHz, THF- d_8): selected resonances δ 8.25 (ddd, $J = 4.8, 1.8, \text{ and } 0.9$ Hz, 1H), 7.42–7.48 (m, 2H), 7.15–7.21 (m, 4H), 6.82–6.85 (m, 1H), 5.65 (d, $J = 5.7$ Hz, 1H), 5.48 (d, $J = 5.7$ Hz, 1H), 5.34 (d, $J = 5.8$ Hz, 1H), 2.72 (sept, $J = 6.8$ Hz, 1H), 2.29 (s, 3H), 1.27 (d, $J = 4.3$ Hz, 3H), 1.25 (d, $J = 4.3$ Hz, 3H), –2.91 (s, 1H) ppm. In addition, the reaction of an orange solution of 5 (0.003 g, 0.006 mmol) with NaBH₄ (4 equivalents) in 0.8 mL of methanol- d_4 gave an orange slightly brown solution. Analysis by NMR showed the Ru-hydride as the major species (52%). 1H NMR (400.1 MHz, Methanol- d_4): selected resonances δ 8.20 (d, $J = 4.8$ Hz, 1H), 7.66 (m, 1H), 7.20–7.29 (m, 4H), 6.95–6.99 (m, 2H), 5.36–5.41 (m, 2H), 2.70 (sept, $J = 7.0$ Hz, 1H), 2.36 (s, 3H), 1.265 (d, $J = 7.0$ Hz, 3H), 1.259 (d, $J = 7.0$ Hz, 3H), –3.04 (s, 1H) ppm.

General procedure for the catalytic reduction of nitroarenes

A standard 20 mL vial was charged with a solution of Ru catalyst (0.003 mmol) in ethanol (2 mL), the appropriate nitroarene (0.3 mmol) and NaBH₄ (0.045 g, 1.2 mmol). The reaction mixture was stirred for 30 min at room temperature. The reaction was quenched with water (2 mL), and the product was extracted with ethyl acetate (3 × 5 mL). The solvent was removed under vacuum, and the obtained residue was dissolved in methanol and analysed by GC-MS. The analytical GC-MS system used was an Agilent 7890A GC coupled to 5975C Mass detector Agilent Technologies, equipped with either a HP-5MS capillary column (30 m × 0.25 mm × 0.25 micron) or a DB-5MS UI capillary column (30 m × 0.25 mm × 0.25 micron) Agilent Technologies, Inc. An Agilent Technologies 7693 auto sampler was used to inject 1 μ L of a sample solution. The ionization energy was 70 eV with a mass range of 30 to 800 m/z . The injector temperature was set at 250 °C and the detector to 230 °C. The flow rate of the carrier gas (helium) was 1.0 mL min^{–1} injected with a gas dilution of 1 : 50. Identification of the individual components was based on comparison with the mass spectra library (NIST08). For substrates nitrobenzene, nitroaniline, nitrophenol and nitrobenzaldehyde the initial column temperature was set at 80 °C, held for 2 min, followed by a ramp of 15 °C min^{–1} to 250 °C. For all other substrates, the initial column temperature was set at 80 °C, held for 2 min, followed by a ramp of 10 °C min^{–1} to 250 °C. Catalytic reactions of entries 9 and 10 in Table 2 were processed according to the general method but with a modification. In these cases, the crude solid obtained after removal of ethanol and water was purified by column chromatography using dichloromethane–methanol (80 : 20) as mobile phase. Removal of solvents under vacuum affords the expected amines. Product of entry 9 is 4-amino-2-(hydroxymethyl)-6-methoxyphenol, brown solid (40 mg, 79%). 1H NMR (400.1 MHz, DMSO- d_6): δ 7.74 (d, $^4J_{HH} = 4.0$ Hz, 1H, Ar), 7.29 (d, $^4J_{HH} = 4$ Hz, 1H, Ar), 5.00 (br s, CH₂OH, 1H), 4.34 (s, 2H, CH₂OH), 3.65 (s, 3H, OCH₃) ppm. Product of entry 10 is 4-amino-2-methoxyphenol, orange solid (33.3 mg, 80%). 1H NMR (400.1 MHz, DMSO- d_6): δ 7.63 (d, $^3J_{HH} = 8.0$ Hz, 1H, Ar), 7.28 (s, 1H, Ar), 5.97 (d, $^3J_{HH} = 8.0$ Hz, 1H, Ar), 3.64 (s, 3H, OCH₃) ppm.

Data availability

The data supporting this article have been included as part of the ESI.†



Author contributions

CRS: investigation, methodology, and visualization. ALI: investigation, methodology, and writing original draft. AVH: investigation. JPCD: investigation. ECA: investigation. JLGL: validation. DC: methodology and formal analysis. AOT: validation. GA: methodology and formal analysis. ALR: methodology and formal analysis. DBG: formal analysis. MPH: formal analysis. VMS: conceptualization, funding acquisition, supervision, writing original draft, reviewing and editing.

Conflicts of interest

There are no conflicts to declare.

Acknowledgements

This research was supported by Tecnológico Nacional de México (TecNM, grants 6185.17P and 14438.22-P) and Consejo Nacional de Ciencia y Tecnología (CONACyT, grant 167005). CRS, AVH, JLGL, and JPCD thank CONACyT for graduate fellowship. We thank CONACyT for ITT NMR, HRMS and X-ray facilities and UNPA HRMS facilities (Grants INFR-2011-3-173395, INFR-2012-01-187686, INFR-2014-224405 and INFR-2015-252013).

Notes and references

- 1 A. S. Travis, Manufacture and uses of the anilines: A vast array of processes and products, in *The Chemistry of Anilines*, ed. Z. Rapport, Patai Series: The Chemistry of Functional Groups, Interscience Wiley, 2007, pp 715–782.
- 2 (a) G. Booth, Nitro Compounds, Aromatics, in *Ullmann's Encyclopedia of Industrial Chemistry*, Wiley-VCH, Verlag GmbH & Co. KGaA, Weinheim, 2012, vol. 24, pp. 301–347; (b) P. F. Vogt, Amines, Aromatic, in *Ullmann's Encyclopedia of Industrial Chemistry*; Wiley-VCH, Verlag GmbH & Co. KGaA, Weinheim, 2012, vol. 2, pp. 699–716.
- 3 Z. Wang, Béchamp Reduction, in *Comprehensive Organic Name Reactions and Reagents*, John Wiley & Sons Inc., 2010, pp. 284–287.
- 4 (a) A. H. Romero, *ChemistrySelect*, 2020, **5**, 13054–13075; (b) J. Song, Z.-F. Huang, L. Pan, K. Li, X. Zhang, L. Wang and J.-J. Zou, *Appl. Catal., B*, 2018, **227**, 386–408; (c) D. Formenti, F. Ferretti, F. K. Scharnagl and M. Beller, *Chem. Rev.*, 2019, **119**, 2611–2680; (d) M. Orlandi, D. Brenna, R. Harms, S. Jost and M. Benaglia, *Org. Process Res. Dev.*, 2018, **22**, 430–445; (e) H. Göksu, H. Sert, B. Kilbas and F. Sen, *Curr. Org. Chem.*, 2017, **21**, 794–820; (f) H. K. Kadam and S. G. Tilve, *RSC Adv.*, 2015, **5**, 83391–83407; (g) H.-U. Blaser, H. Steiner and M. Studer, *ChemCatChem*, 2009, **1**, 210–221.
- 5 (a) J. Wu and C. Darcel, *J. Org. Chem.*, 2021, **86**, 1023–1026; (b) G. Wienhofer, M. Baseda-Kruger, C. Ziebart, F. A. Westerhaus, W. Baumann, R. Jackstell, K. Junge and M. Beller, *Chem. Commun.*, 2013, **49**, 9089–9091; (c) R. M. Deshpande, A. N. Mahajan, M. M. Diwakar, P. S. Ozarde and R. V. Chaudhari, *J. Org. Chem.*, 2004, **69**, 4835–4838.
- 6 (a) D. I. Ioannou, D. K. Giftoisidou, V. E. Tsina, M. G. Kallitsakis, A. G. Hatzidimitriou, M. A. Terzidis, P. A. Angaridis and I. N. Lykakis, *J. Org. Chem.*, 2021, **86**, 2895–2906; (b) S. Kumar and R. Gupta, *ChemistrySelect*, 2017, **2**, 8197–8206; (c) C.-G. Chao and D. E. Bergbreiter, *Catal. Commun.*, 2016, **77**, 89–93.
- 7 (a) S. Dayan, N. Kayacıb, O. Dayan, N. Özdemir and K. N. Özpozan, *Polyhedron*, 2020, **175**, 114181; (b) R. Lopes, M. Pereira and B. Royo, *ChemCatChem*, 2017, **9**, 3073–3077; (c) G. Vijaykumar and S. K. Mandal, *Dalton Trans.*, 2016, **45**, 7421–7426.
- 8 (a) S. Liu, J. I. Amaro-Estrada, M. Baltrun, I. Douair, R. Schoch, L. Maron and S. Hohloch, *Organometallics*, 2021, **40**, 107–118; (b) I. Sorribes, G. Wienhöfer, C. Vicent, K. Junge, R. Llugar and M. Beller, *Angew. Chem., Int. Ed.*, 2012, **51**, 7794–7798.
- 9 V. Zubar, A. Dewanji and M. Rueping, *Org. Lett.*, 2021, **23**, 2742–2747.
- 10 (a) N. Zengin, H. Göksu and F. Şen, *Chemosphere*, 2021, **282**, 130887; (b) S. T. Yang, P. Shen, B. S. Liao, Y. H. Liu, S. M. Peng and S. T. Liu, *Organometallics*, 2017, **36**, 3110–3116; (c) A. Krogul and G. Litwinienko, *Org. Process Res. Dev.*, 2015, **19**, 2017–2021; (d) A. Kumar, K. Purkait, S. K. Dey, A. Sarkar and A. Mukherjee, *RSC Adv.*, 2014, **4**, 35233–35237.
- 11 Y. Liu, W. Miao, W. Tang, D. Xue, J. Xiao, C. Wang and C. Li, *Chem.-Asian J.*, 2021, **16**, 1725.
- 12 (a) S. Pachisia, R. Kishan, S. Yadav and R. Gupta, *Inorg. Chem.*, 2021, **60**, 2009–2022; (b) R. Saha, A. Mukherjee and S. Bhattacharya, *Eur. J. Inorg. Chem.*, 2020, 4539–4548; (c) R. Nandhini, B. S. Krishnamoorthy and G. Venkatachalam, *J. Organomet. Chem.*, 2019, **903**, 120984; (d) Z.-J. Yao, J.-W. Zhu, N. Lin, X.-C. Qiao and W. Deng, *Dalton Trans.*, 2019, **48**, 7158–7166; (e) S.-C. A. Lin, Y.-H. Liu, S.-M. Peng and S.-T. Liu, *Mol. Catal.*, 2019, **466**, 46–51; (f) W.-G. Jia, S. Ling, H.-N. Zhang, E.-H. Sheng and R. Lee, *Organometallics*, 2018, **37**, 40–47; (g) W.-G. Jia, Z.-B. Wang, X.-T. Zhi, J.-Q. Han and Y. Sun, *J. Coord. Chem.*, 2017, **70**, 848–858; (h) W.-G. Jia, T. Zhang, D. Xie, Q.-T. Xu, S. Ling and Q. Zhang, *Dalton Trans.*, 2016, **45**, 14230–14237; (i) W.-G. Jia, H. Zhang, T. Zhang, D. Xie, S. Ling and E.-H. Sheng, *Organometallics*, 2016, **35**, 503–512; (j) S. Hohloch, L. Suntrup and B. Sarkar, *Organometallics*, 2013, **32**(24), 7376–7385; (k) A. A. Deshmukh, A. K. Prashar, A. K. Kinage, R. Kumar and R. Meijboom, *Ind. Eng. Chem. Res.*, 2010, **49**, 12180–12184.
- 13 (a) L. J. Medrano-Castillo, M. A. Collazo-Flores, J. P. Camarena-Díaz, E. Correa-Ayala, D. Chávez, D. B. Grotjahn, A. L. Rheingold, V. Miranda-Soto and M. Parra-Hake, *Inorg. Chim. Acta*, 2020, **507**, 119551; (b) J. P. Camarena-Díaz, A. L. Iglesias, D. Chávez, G. Aguirre, D. B. Grotjahn, A. L. Rheingold, M. Parra-Hake and V. Miranda-Soto, *Organometallics*, 2019, **38**, 844–851; (c) E. Correa-Ayala, C. Campos-Alvarado, D. Chávez, D. Morales-Morales, S. Hernández-Ortega, J. J. García,



- M. Flores-Álamo, V. Miranda-Soto and M. Parra-Hake, *Inorg. Chim. Acta*, 2017, **466**, 510–519; (d) E. Correa-Ayala, A. Valle-Delgado, G. Ríos-Moreno, D. Chávez, D. Morales-Morales, S. Hernández-Ortega, J. J. García, M. Flores-Álamo, V. Miranda-Soto and M. Parra-Hake, *Inorg. Chim. Acta*, 2016, **446**, 161–168.
- 14 (a) A. E. Chichibábin and R. L. Persitz, *J. Russ. Phys.-Chem. Soc.*, 1925, **57**, 301–304; (b) G. Vernin, C. Siv, J. Metzger and C. Párkányi, *Synthesis*, 1977, **10**, 691–693.
- 15 A. Messmer, A. Gelléri and G. Hajós, *Tetrahedron*, 1986, **42**, 4827–4836.
- 16 (a) D. Lee, P. Perez, W. Jackson, T. Chin, M. Galbreath, F. R. Fronczek, R. Isovitsch and D. S. Limoto, *Bioorg. Med. Chem. Lett.*, 2016, **26**, 3243–3247; (b) M. F. Ibárra-Vázquez, S. A. Cortes-Llamas, A. A. Peregrina-Lucano, J. G. Alvarado-Rodríguez, R. Marriquéz-González, F. A. López-Dellamary, M. I. Moreno-Brambila and I. I. Rangel-Salas, *Inorg. Chim. Acta*, 2016, **451**, 209–215; (c) C. GuhaRoy, R. J. Butcher and S. Bhattacharya, *J. Organomet. Chem.*, 2008, **693**, 3923–3931; (d) S. Antoniutti, M. Bedin, J. Castro, S. García-Fontana and G. Albertin, *Inorg. Chem.*, 2006, **45**, 3816–3825.
- 17 (a) Y. Hu, L. Li, A. P. Shaw, J. R. Norton, W. Sattler and Y. Rong, *Organometallics*, 2012, **31**, 5058–5064; (b) K. Gray, M. J. Page, J. Wagler and B. A. Messerle, *Organometallics*, 2012, **31**, 6270–6277.
- 18 (a) J. Vajs, I. Steiner, A. Brozovic, A. Pevec, A. Ambriović-Ristov, M. Matković, I. Piantanida, D. Urankar, M. Osmak and J. Košmrlj, *J. Inorg. Biochem.*, 2015, **153**, 42–48; (b) G. Albertin, S. Antoniutti, J. Castro and S. Paganelli, *J. Organomet. Chem.*, 2010, **695**, 2142–2152; (c) M. C. Carrión, F. Sepúlveda, F. A. Jalón, B. R. Manzano and A. M. Rodríguez, *Organometallics*, 2009, **28**, 3822–3833.
- 19 P. Bhaskar, K. Chakrabarti, S. Shee, M. Maji, A. Mishra and S. Kundu, *RSC Adv.*, 2016, **6**, 100532–100545.
- 20 (a) W. Jia, T. Du, L. Gao and J. Du, *Appl. Organomet. Chem.*, 2016, **34**, e5651; (b) J. Wei-Guo, C. Ming-Xia, X. Qiu-Tong, G. Li-Li and Y. Guozan, *Polyhedron*, 2018, **153**, 69–75; (c) M. Pietrowski, *Curr. Org. Synth.*, 2012, **9**, 470–487.
- 21 M. A. Bennett, T. N. Huang, T. W. Matheson, A. K. Smith, S. Ittel and W. Nickerson, *Inorg. Synth.*, 1982, **21**, 74.

